

See discussions, stats, and author profiles for this publication at: <https://www.researchgate.net/publication/314016886>

Optimizing grain size distribution in Nd:YVO₄ powder pellets for random laser action with 5% slope efficiency

Conference Paper · February 2017

DOI: 10.1117/12.2256600

CITATIONS

0

READS

16

5 authors, including:



N.U. Wetter

Instituto de Pesquisas Energéticas e Nucleares

183 PUBLICATIONS 1,414 CITATIONS

[SEE PROFILE](#)



Ernesto Jiménez-Villar

University of Valencia

64 PUBLICATIONS 353 CITATIONS

[SEE PROFILE](#)

Some of the authors of this publication are also working on these related projects:



Hydroxylapatite coating for medical implants [View project](#)



Photonics in disorder media [View project](#)

Optimizing grain size distribution in Nd:YVO₄ powder pellets for random laser action with high efficiency

Niklaus U. Wetter^{*a}, E. Jimenez-Villar^b, Julia M. Ghies^a, Felix Butzbach^a, Victor Tayra^a,
^aCentro de Lasers e Aplicações, IPEN-CNEN/SP, Av. Prof. Lineu Preses, 2242, 05508-000 São Paulo, Brazil; ^bDepartamento de Química Fundamental, Universidade Federal de Pernambuco, Recife, 50670-901, Brazil

ABSTRACT

We demonstrate a volumetric random laser with an optical efficiency of 15%. We use a 1.33 mol% Nd:YVO₄ crystal, grind it and mix the particles into ten different size distributions with mean particle sizes ranging from approximately 10 micrometers to 100 micrometers. After pressing into pellets, each of the ten groups has its transport mean free path calculated from the distribution spectra and experimentally measured by means of its backscattering cone. We then calculate the fill fractions of each sample. The pellets are diode-pumped at 806.5 nm. Linewidth narrowing and output power are measured as a function of absorbed pump power. We demonstrate that the smaller particles, trapped between large particles, serve as gain centers whereas the large particles control the light diffusion into the sample. By optimizing diffusion and gain we achieve high slope efficiency.

Keywords: materials, scattering particles, laser materials, random lasers, backscattering

1. INTRODUCTION

Random lasers^{1,2} (RL) exist since the 1960s and find nowadays important applications, such as speckle-free imaging in biology, remote-sensing, display technology, encrypting, cancer detection and distributed amplification^{3,4}. A major advantage of RLs over regular lasers is that their production is cheap, the required technology relatively simple and it is possible to produce RLs with several different materials like semiconductor nanoparticles, ceramic powders, polymers, organic materials and biological tissues^{5,6,7}. Potential applications require optimization of RL performance with respect to laser efficiency. Only when random lasers achieve efficiency comparable to traditional lasers will their inherent cost advantages become attractive for the large majority of applications.

M. A. Noginov et al. have studied the dependence of RL emission in neodymium doped powders (Nd_{0.5}La_{0.5}Al₃(BO₃)₄) on the particle size, the powder volume density and the pump spot size^{8,9,10}. Best reported efficiency was below half a percent. An impediment for increasing the efficiency is the surface reflectivity of the compacted powders. The reflection coefficient of Nd_{0.5}La_{0.5}Al₃(BO₃)₄ at $\lambda = 532$ nm for medium to high powder density is approximately 0.5⁹. Using a fiber-coupled random laser, where the pump fiber terminates deep inside the scattering medium in order to deliver the pump energy directly into the gain volume without reflection loss at the surface, Noginov et al. achieved a higher efficiency of approximately 0.7%¹¹.

The stimulated RL emission of these rare earth doped powder pellets comes in the form of a Lambertian emission¹² with a linewidth that decreases around laser threshold and becomes much smaller than typical ASE emission. Output power also shows a typical laser threshold and slope efficiency. As we have shown¹³ for Nd:YVO₄, the emission decay after a pump pulse, follows two different exponentials corresponding to a fast laser emission decay of a few microseconds and a slower fluorescence emission decay which is shorter than the intrinsic decay time, which should amount to 73 μ s for 1.33mol% neodymium doping concentration, because of up conversion. We therefore expected some decrease in laser efficiency due energy transfer up conversion.

* nuwetter@ipen.br; phone 55 11 31339359; www.ipen.br

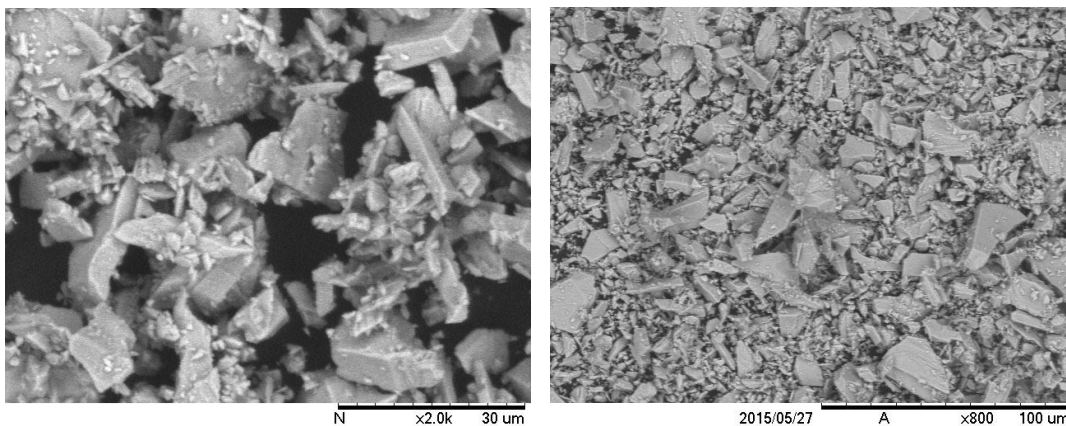
To further increase the efficiency of the random laser we propose a system composed of mixed grains: grains of diameter of tens microns and grains with smaller diameters in order to occupy the void space between the bigger particles. The system has high volume fraction of large grains, which we control by using different mesh sizes ranging from 10 μm to 180 μm , and a small volume fraction of much smaller grains. Although these smaller grains represent only a few percent of the volume, in terms of numbers they make up the majority of the particles. These small particles which are trapped in between the big particles create regions with very short transport mean free path and therefore concentrate the light. As a consequence, the absorption mean free length within these regions is much smaller than within the bigger particles, therefore, these regions must act as gain centers inside the random laser.

On the other hand, the coherent emission of the random laser originates from a volume that corresponds in depth to several times the transport mean free path. This volume is determined by larger particles that govern the macroscopic diffusion properties of light inside the samples. By adjusting the volume fraction of each particle size inside the same sample we could effectively control separately the mechanisms of gain and diffusion thereby optimizing the output efficiency of this new type of random laser. In this work we use a method of sample preparation that gives us some control and demonstrate as a result of this procedure a more than two fold increase in laser efficiency.

2. POWDER PREPARATION

In order to achieve a powder with a high gain coefficient, necessary for highly efficiency laser action, we used a $\text{Nd}^{3+}:\text{YVO}_4$ (yttrium vanadate doped with neodymium) crystal, known for its excellent performance in diode pumped solid state lasers¹⁴. There are a series of other laser crystals which result in similar efficiencies^{15,16} when used in traditional standing wave cavities such as $\text{Nd}:\text{YAG}$ and $\text{Nd}:\text{YLF}$ ^{17,18}, however, for a random laser, several cavity parameters are random or cannot be determined and therefore we concentrate on one of the controllable parameters, which is the absorption coefficient. The typical absorption coefficient for $\text{Nd}:\text{YVO}_4$ is very high, approximately 60 cm^{-1} for 1 mol% neodymium doping. We also tried materials based on binary glasses¹⁹ with lower absorption coefficient but without success. In order to further enhance the absorption we used a YVO crystal with 1.33 mol% neodymium doping, which results in a ballistic absorption coefficient of 80 cm^{-1} for the bulk crystal.

Pieces of the $\text{Nd}:\text{YVO}_4$ crystal were grinded and the powder sieved by means of differently sized mesh grids to obtain ranges of different particle sizes (see table 1). The mesh grids ranged from a 10 μm mesh to a 180 μm mesh. When observed beneath the microscope, the powders were not monodispersed. On the contrary, a large quantity of smaller particles adhered to the large particles retained by the sieve. We therefore used a cleansing procedure with the objective to get better monodispersed powders. This procedure consisted of mixing isopropyl alcohol with the powders, stirring the liquid for 5 minutes using ultrasound, then sieving again and drying for a period of 24 hours. The result was satisfactory for the larger grain sizes, however, for particles less than 20 μm , the powder still consisted of a mixture of large and small particles. This behavior can be observed in Figure 1. A total of three powder samples were prepared for each group. Each of the powder samples was characterized separately.



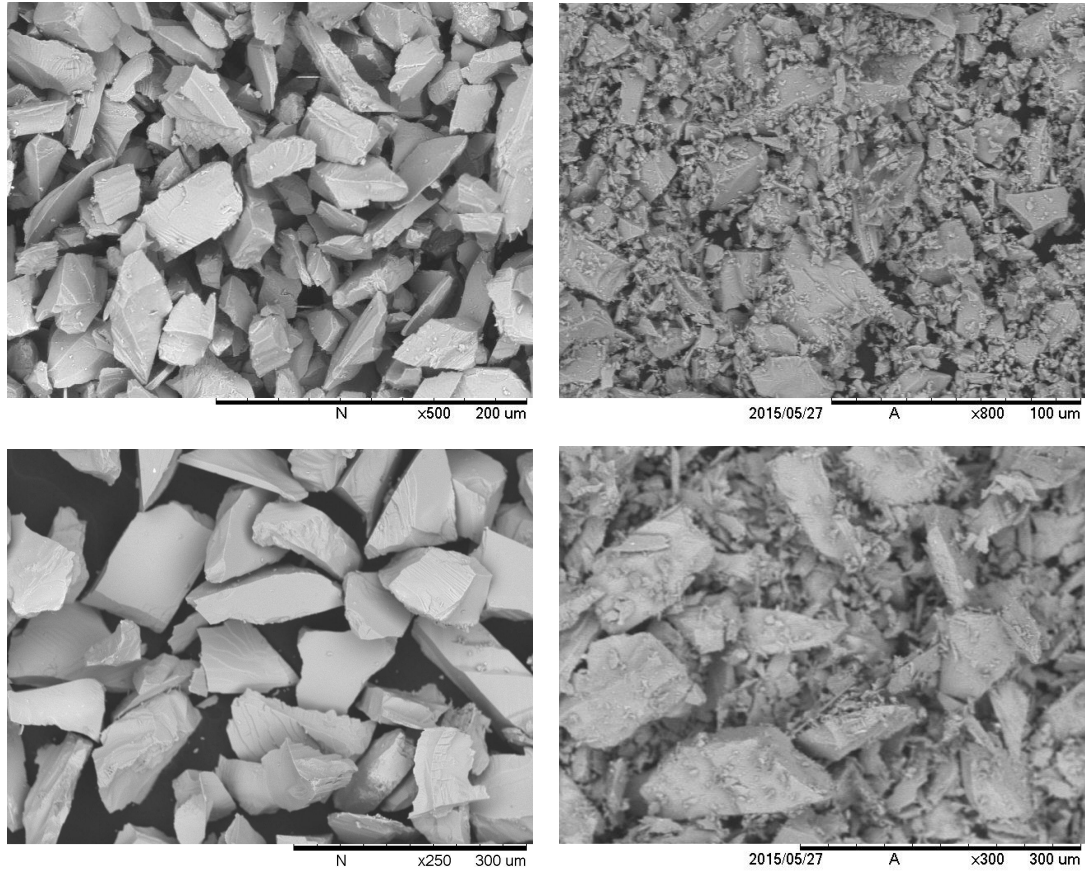


Figure 1: SEM images of $\text{Nd}^{3+}:\text{YVO}_4$ powders from cleansed samples (left column) and mixed samples (right column). The images in the first row are from samples of group 1 (B1 and A1, respectively), the second row contains images from B2 and A2, respectively, and the last row B4 and A4. It can be observed that the cleansed samples are much more monodispersed except for the first group B1, that contains a considerable fraction of smaller particles.

3. POWDER CHARACTERIZATION

In order to characterize the grain size distribution in each sample we used the Fraunhofer Laser diffraction technique (model CILAS 930), which is appropriate, given the fact that our sieves retained mainly particles between $10\ \mu\text{m}$ and $500\ \mu\text{m}$. As we shall see, errors occur for some of the non-cleansed powder groups and the cleansed powder group B1 shows also some error. For these groups, which contain a large fraction of small particles (less than $1\ \mu\text{m}$), the Mie calculation might give better results, however, this error should be less than 30%²⁰. The result of the Fraunhofer diffraction technique comes in the form of a table containing about 100 classes of different particle diameters and the respective population density. The average of the three powder samples of each group was used to calculate the mean diameter and the standard deviation by means of a MATLAB program, which was also used to calculate the scattering cross-section and transport means free path of each group.

In Figure 2, each graph represents one of the three powder samples that were analyzed for each of the groups. It can be observed again that the cleansing procedure (left column) works well for the groups B2 and B4 and less for group B1. The respective mixed samples present all a higher percentage of small particles, which is shown in part by the characteristic shoulder to the left of the histogram peak (right column).

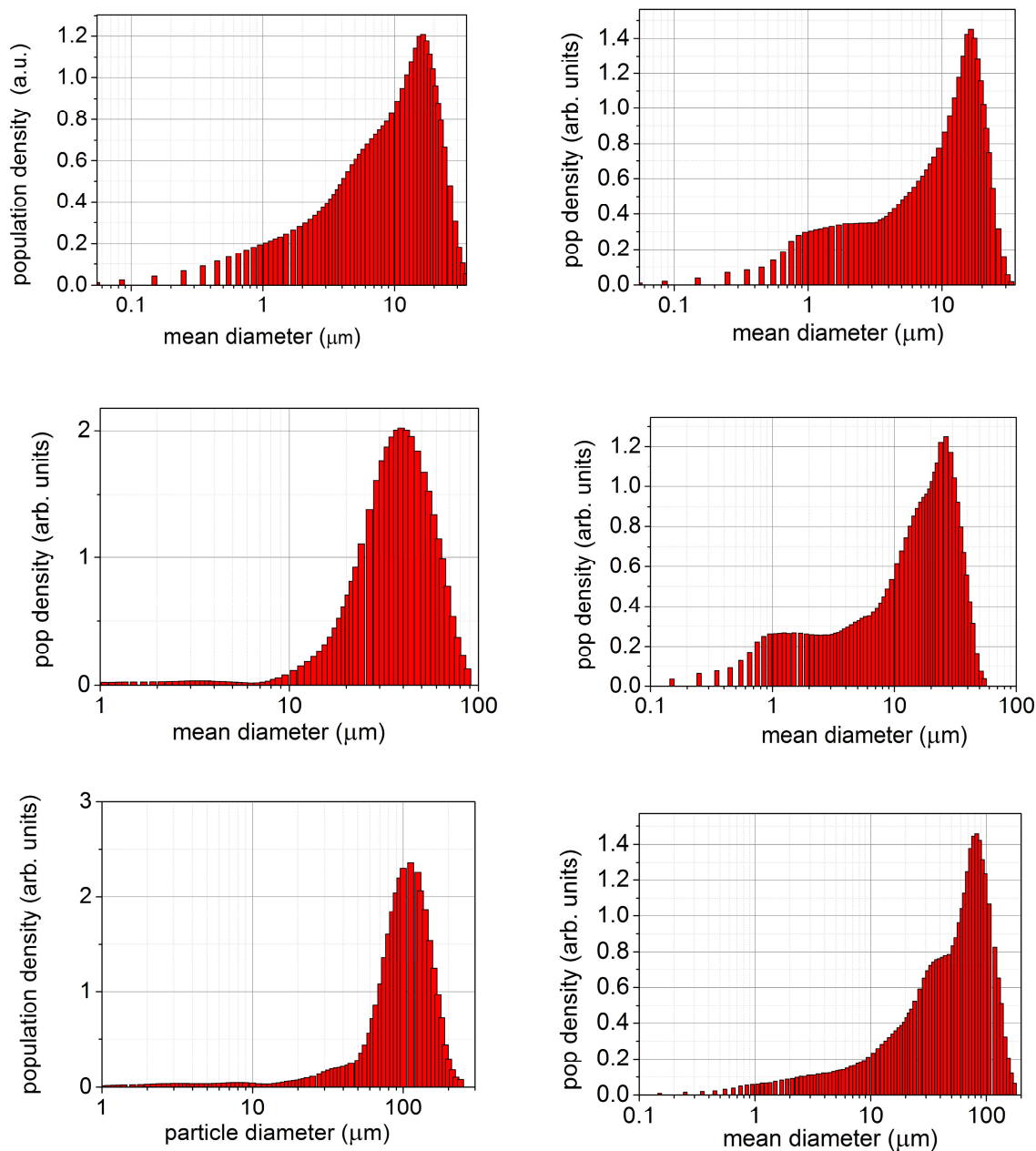


Figure 2: a) histogram of population density in volume from mixed samples of group A (right column) and cleansed samples B (left column). The order is the same as in Figure 1: The images in the first row are from samples of group 1 (B1 and A1, respectively), the second row contains images from B2 and A2, respectively, and the last row B4 and A4.

Table 1 shows the main result of this section. Observed is the strong participation of smaller particles in the A groups when comparing their mean particle sizes with their cleansed counterpart: in all cases the A groups show smaller mean diameters. Also clearly seen is the much larger standard deviation (SD) of the mixed groups when compared to the cleansed groups. Main particle size of group B₅ was obtained by SEM image analysis because the high quantity of large particles caused errors to the results produced by the CILAS equipment and because it is simple to count large monodispersed particles by SEM analysis.

Table 1: Groups of powder grain size distributions for the mixed Nd³⁺:YVO₄ powders. Standard deviation (SD) is only calculated for the groups shown in Figure 1 and Figure 2.

mesh grid interval (μm)	mixed powders groups A		SD	cleansed powders groups B		SD
		mean particle size			mean particle size	
10 – 20	A ₁	9.5 μm	7.3	B ₁	9.9 μm	0.98
20 - 45	A ₂	15 μm	12	B ₂	37 μm	2.17
45 - 75	A ₃	30 μm	-	B ₃	55 μm	-
75 - 106	A ₄	54 μm	39	B ₄	96 μm	4.7
106 - 180	A ₅	125 μm	-	B ₅	*147μm	-

After characterization were produced using approximately 60 mg of powder and a pressure of 255 MPa. The pellet's diameter was 5 mm and their thickness approximately 1 mm. Per group, three pellets were produced on average. Some of these pellets did not withstand handling, especially for the large grain sizes.

4. CALCULATION AND MEASUREMENT OF THE TRANSPORT MEAN FREE PATH

With the measured grain size distributions (Figure 2) we calculated the scattering cross sections of the samples for a fill fraction of 1, using the above mentioned MATLAB program, whose code was based on free optics software²¹.

A set-up for measuring the transport mean free path was installed²², as shown in Figure 3. A 30 mW HeNe laser ($\lambda = 632.8$ nm) was first polarized in the vertical direction by a polarizer cube and its beam diameter was expanded to 5 mm in order to illuminate a larger area of the sample, which improves the resolution of the set-up. A modified Michelson interferometer configuration was employed to detect the backscattered intensity coming from the sample. The sample is fixed on a motor rotating at a speed of ~50 Hz in order to ensemble average the speckles coming from the sample surface. The sample was tilted 15 degrees in order to remove unwanted Fresnel reflection (more than 15 degrees results in a change of the width of the backscattering cone). The backscattered light went through an analyzer, in order to measure the vertical polarization-conserving channel, thereby eliminating single scattering events. The backscattered light was focused onto a CCD camera using either first a $f = 150$ mm and later a $f = 50$ mm lens. The use of two set-ups using different focusing lenses was to improve the precision of the measurement. The longer focal length gives higher precision for the center of the backscattering cone whereas the smaller focal length gives better precision for the wings of the backscattering cone.

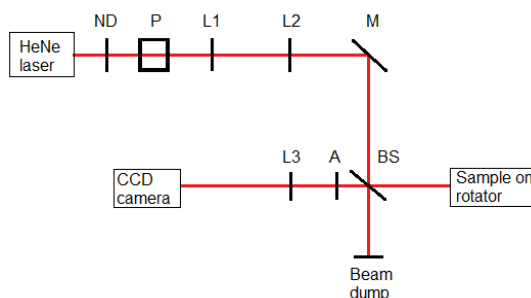


Figure 3: Set-up used to measure coherent backscattering intensity profiles. ND is variable neutral density filter; P is a polarizer cube; M is a gold-coated mirror; BS is a 50% beam splitter (632.8 nm); A is an analyzer; L1, L2 and L3 are lenses with focal lengths of 50 mm, 200 mm and 50 mm (or 150 mm), respectively.

The images of the coherent backscattering cone were adjusted to a theoretical fit, given in references^{23,24,25}, and the transport mean free path l_t , which is inversely proportional to the full width at half maximum of the fitted CBS cone, was calculated from the following equation:

$$l_t = \frac{0.35 * (\lambda \cdot 0.7)}{2 \cdot \pi \cdot \text{FWHM}} \quad (1)$$

where the factor of 0.35 is a correction for the sample's reflectivity at 632 nm^{26,27}.

Surface reflectivity was measured at 705 nm (zero absorption of neodymium ions) and absorption was measured at 805 nm (absorption peak of neodymium) using a spectrometer with a calibrated integrating sphere (Agilent Technologies, model CARY-5000).

4.1 Results

The results are compiled in Table 2. They are separated into measured and calculated columns, where the former means the results obtained by the backscattering cone measurements and the later means the results obtained by computation from the particle size distribution measurements. The difference between both results is attributed to the filling factor, because our calculated results assume a filling factor of unity.

Table 2: Transport mean free path. Measured results are using the backscattering cone set-up and calculated results are obtained with the MATLAB code using the particle size distribution measurements.

mixed powders groups A			cleansed powders groups B		
group	measured (μm)	calculated (μm)	group	measured (μm)	calculated (μm)
A ₁	1.4	0.66	B ₁	2.4	0.7
A ₂	2.1	0.77	B ₂	2.6	2.2
A ₃	2.8	0.7	B ₃	3.2	2.4
A ₄	3.1	2.52	B ₄	4.6	2.8
A ₅	4.6	3	B ₅	5.2	3.0

As expected, the mixed groups always show smaller transport mean free path. A large difference between both columns of each set of groups (A and B) is observed whenever the calculated transport mean free path is below 1 μm . We attribute this effect to the presence of agglomerates of smaller particles (close to or less than a wavelength) in the pressed pellets. These agglomerates influence the measurements of the backscattering cone returning a larger transport mean free path, since these agglomerates scatter the light as a single particle with bigger diameter.

If we exclude the samples where the calculated transport mean free path is below 1 μm we obtain results for the filling fraction by dividing calculated results by measured results (bold numbers in Table 3). Whenever smaller particles are present (groups A), these particles fill the voids between the larger particles and increase the fill fraction. The more monodispersed the samples are the lower the fill fraction, which in turn should be less than for closely packed and monodispersed spheres that would occupy 74% of the volume, given that our samples consist of elongated irregular chunks of material.

Table 3: Fill fraction as obtained from the measured and calculated transport mean free path.

mixed powders groups A				cleansed powders groups B			
group	measured (μm)	calculated (μm)	fill fraction	group	measured (μm)	calculated (μm)	fill fraction
A ₂	-	-	-	B ₂	2.6	2.2	0.84615
A ₃	-	-	-	B ₃	3.2	2.4	0.75
A ₄	3.1	2.52	0.81	B ₄	4.6	2.8	0.6087
A ₅	4.6	3	0.65	B ₅	5.2	3.0	0.57692

5. LASER CHARACTERIZATION

The pellets were pumped using a laser diode in quasi-continuous regime operating at 808 nm with 5 Hz repetition rate and 150 μs pulse width. The experimental setup is shown in Figure 4. The pump beam size was made as small as possible to increase the laser pump intensity in order to achieve a low threshold for laser action.

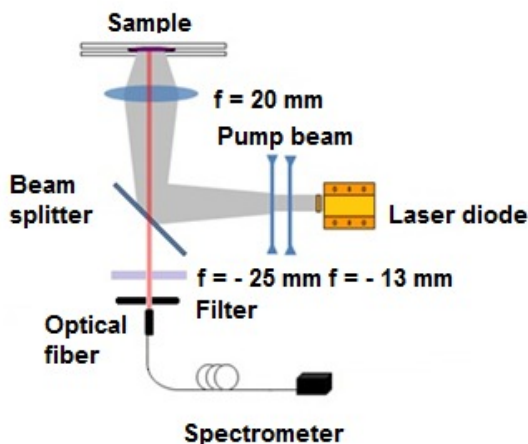


Figure 4: Experimental setup: The diode beam is first expanded in the vertical direction by two cylindrical lenses with focal lengths of -13 mm and -25 mm , respectively, and then focused onto the sample with a spherical lens $f = 20\text{ mm}$. A dichroic beam splitter separates the pump wavelength from the laser emission. A neutral density filter was placed in front of the optical fiber to attenuate the laser measured in the backscattered direction.

The setup consisted of a diode laser whose beam was first expanded in the vertical direction by two cylindrical lenses of focal length -13 and -15 mm , respectively, in order to achieve an approximately square shaped focus at the sample position of $2 \times 2\text{ mm}$. A dichroic beam splitter highly reflective at 808 nm and with 80% transmission at 1064 nm , separated the pump from the random laser emission. A spherical lens of 20 mm focal length was used for focusing the pump beam on the sample and a neutral density filter was inserted before the detector. An optical fiber connected spectrometer (Ocean Optics model HR 2000) with 0.11 nm resolution was used for spectral data acquisition. For pump energy measurements a high power energy detector was used (COHERENT Field Master GS Laser) whereas a low power pyroelectric energy sensor with resolution of 100 nJ (Thorlabs ES111C) was positioned behind the beamsplitter for random laser power measurements.

The overall highest output power was achieved for the mixed sample A₄. With a pump pulse duration of 150 μs and maximum pump power of 55 W, resulting in a measured pulse energy of $E_{\text{meas}} = 8.2$ mJ at the pellet location, we achieved an output energy of 130 μJ at 1064 nm as shown in Figure 5. This measurement was done with the focusing lens at a distance D of 35 mm from the sample surface. Given the lens's free aperture of $r = 11.5$ mm radius, we calculate a collection angle of 36 degrees. Assuming a Lambertian emission and neglecting the contribution from the coherent backscattering cone, the total output power can be calculated by $E_{\text{out}} = (D/r)^2 E_{\text{meas}}$, which correspond to 1.2 mJ or 15% optical efficiency with respect to pump power.

The highest output power for the cleansed samples was achieved with sample B₃. Both groups showed similar mean particle size of approximately 55 μm, which results in similar transport mean free paths (around 3μm). In order to compare the effect of smaller particles on the random laser action, figure 5 shows a comparison of the linewidth and output power for both samples (B₃ and A₄). The A₄ sample showed a 2.6 times higher output power, revealing that the smaller particles improve the RL performance.

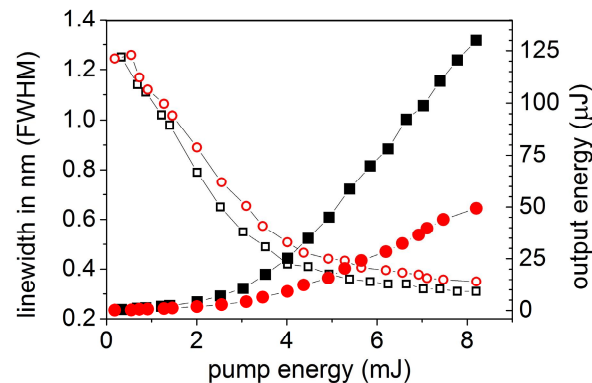


Figure 5: linewidth narrowing (left axis; open symbols) and output power (right axis; full symbols) for the cleansed group B₃ (circles) and the mixed group A₄ (squares).

When comparing other groups within the same class (mixed or cleansed) the output power decreases slowly, approximately 20%, for the next larger group (A₅ or B₄) and much faster for the next smaller group (A₃ or B₂; more than 50%). No linewidth narrowing was observed for a test sample that had only particles less than 10 μm.

6. CONCLUSIONS

In this manuscript, we demonstrated that the most efficient random laser action is achieved for samples containing a mean particle size of approximately 55 μm (groups A₄ or B₃). Both samples show similar calculated and measured transport mean free path. However, the random laser efficiency of the mixed sample is 160% higher than the cleansed (monodispersed) sample. This indicates that the smaller particles, placed within the void spaces between the bigger particles, play a crucial role in improving the random laser performance.

REFERENCES

- [1] Letokhov, V. S., "Stimulated emission of an ensemble of scattering particles with negative absorption," *JETP Lett.* **5**, 212-215 (1967).
- [2] Letokhov, V. S., "Generation of light by a scattering medium with negative resonance absorption," *Sov. Phys. JETP* **26**, 835-840 (1968).
- [3] Polson, R.C., Vardenya, Z.V., "Random lasing in human tissues." *Appl. Phys. Lett.* **85**, 1289–1291 (2004).
- [4] Redding, B., Choma, M. A., Cao, H., "Speckle-free laser imaging using random laser illumination," *Nat. Photonics* **6**, 355-359 (2012).

- [5] Cao, H., Zhao, Y. G., Ho, S. T., Seelig, E. W., Wang, Q. H. and Chang, R. P. H., "Random Laser Action in Semiconductor Powder," *Phys. Rev. Lett.* **82**, 2278-2281 (1999).
- [6] Polson, R. C., Chipouline, A., Vardeny, Z. V., "Random Lasing in π -Conjugated Films and Infiltrated Opals," *Adv. Mater.* **13**, 760-764 (2001).
- [7] Wiersma, D. S., "The physics and applications of random lasers," *Nat. Phys.* **4**, 359-367 (2008).
- [8] Bahoura, M., Morris, K. J., Zhu, G. and Noginov, M. A., "Dependence of the neodymium random laser threshold on the diameter of the pumped spot," *IEEE J. Quantum Electron.* **41**(5), 677-685 (2005).
- [9] Noginov, M. A., Noginova, N. E., Egarievwe, S. U., Caulfield, H. J., Cochrane, C., Wang, J. C., Kokta, M. R., Paitz, J., "Study of the pumping regimes in Ti-sapphire and $\text{Nd}_{0.5}\text{La}_{0.5}\text{Al}_3(\text{BO}_3)_4$ powders," *Opt. Mat.* **10**, 297-303 (1998).
- [10] Bahoura, M., Morris, K. J., Noginov, M. A., "Threshold and slope efficiency of $\text{Nd}_{0.5}\text{La}_{0.5}\text{Al}_3(\text{BO}_3)_4$ ceramic random laser: effect of the pumped spot size," *Opt. Com.* **201**, 405-411 (2002).
- [11] Noginov, M. A., Fowlkes, I. N., and Zhu, G., "Fiber-coupled random laser," *Appl. Phys. Lett.* **86**, 161105/1-5 (2005).
- [12] Noginov, M. A., Noginova, N. E., Egarievwe, S. U., Caulfield, H. J., Venkateswarlu, P., Williams, A. and Mirov, S. B., "Color-center powder laser: The effect of pulverization on color-center characteristics," *J. Opt. Soc. Am. B* **14**(8), 2153-2160 (1997).
- [13] Vieira, R. J. R., Gomes, L., Martinelli, J. R. and Wetter, N. U., "Upconversion luminescence and decay kinetics in a diode-pumped nanocrystalline $\text{Nd}^{3+}:\text{YVO}_4$ random laser," *Opt. Express* **20**, 12487-12497 (2012).
- [14] Wetter, N., Camargo, F. and Sousa, E., "Mode-controlling in a 7.5 cm long, transversally pumped, high power $\text{Nd}:\text{YVO}_4$ laser," *J. Opt. A: Pure Appl. Opt.* **10**, 104012 (2008).
- [15] Wetter, N. U., Deana, A. M., "Influence of pump bandwidth on the efficiency of side-pumped, double-beam mode-controlled lasers: establishing a new record for $\text{Nd}:\text{YLiF}_4$ lasers using VBG," *Opt. Express* **23**, 9279-9287 (2015).
- [16] Wetter, N. U., Sousa, E. C., Ranieri, I. M., Baldochi, S. L., "Compact, diode-side-pumped $\text{Nd}^{3+}:\text{YLiF}_4$ laser at 1053 nm with 45% efficiency and diffraction-limited quality by mode controlling," *Opt. Lett.* **34**, 292-294 (2009).
- [17] Wetter, N. U., Sousa, E. C., Camargo, F. D., Ranieri, I. M., Baldochi, S. L., "Efficient and compact diode-side-pumped $\text{Nd}:\text{YLF}$ laser operating at 1053 nm with high beam quality," *J. Opt. A: Pure Appl. Opt.* **10**, 104013 (2008).
- [18] Jakutis-Neto, J., Lin, J. P., Wetter, N. U., Pask, H., "Continuous-wave watt-level $\text{Nd}:\text{YLF}/\text{KGW}$ Raman laser operating at near-IR, yellow and lime-green wavelengths," *Opt. Express* **20**, 9841-9850 (2012).
- [19] de Assumpção, T. A. A., Kassab, L. R. P., Gomes, A. S. L., de Araújo, C. B., Wetter, N. U., "Influence of the heat treatment on the nucleation of silver nanoparticles in Tm^{3+} doped PbO-GeO_2 glasses," *Appl. Phys. B* **103**, 165-169 (2011).
- [20] Jones, A. R., "Error contour charts relevant to particle sizing by forward-scattered lobe methods," *J. Phys. D: Appl. Phys.* **10**, 138-140 (1977).
- [21] Prahl, S., "Mie Theorie," (2007) <http://www.omlc.org/software/>
- [22] Ghil, J. M., Butzbach, F., Jorge, K. C., Alvarado, M. A., Carreno, M. N. P., Alayo, M. I., Wetter, N. U., "Random lasers for lab-on-chip applications," *Proc. SPIE* **9893**, 989314-8 (2016).
- [23] Akkermans, E., Wolf, P. E. and Maynard, R., "Coherent backscattering of light by disordered media: analysis of the peak line shape," *Phys. Rev. Letters* **56**, 1471-1474 (1986).
- [24] Bahoura, M. and Noginov, M. A., "Determination of the transport mean free path in a solid-state random laser," *J. Opt. Soc. Am. B* **20**, 2389-2394 (2003).
- [25] Giehl, J., Miranda, A., Reijn, S., Butzbach, F. and Wetter, N., "Relationship between coherent backscattering cone and the study of the random laser emission of $\text{Nd}^{3+}:\text{YVO}_4$ powders changing the particle size and applied pressure," in *Advanced Solid State Lasers, OSA Technical Digest (Optical Society of America)*, paper ATu2A.4 (2014).
- [26] van der Mark, M. B., van Albada, M. P., Lagendijk, A., "Light scattering in strongly scattering media: Multiple scattering and weak localization," *Phys. Rev. B* **37**, 3575-3592 (1988).
- [27] Lagendijk, A., Vreeker, R. and De Vries, P., "Influence of internal reflection on diffusive transport in strongly scattering media," *Phys. Lett. A* **136**, 81-88 (1989).